Fibrillated Cellulose on Lime Pastes and Mortars

Subjects: Agricultural Engineering

Contributor: Chiara D'erme

The use of nanocellulose in traditional lime-based mortars is a promising solution for green buildings in the frame of limiting the CO2 emissions resulting from Portland Cement production. The influence of the fibrillated cellulose (FC) on lime pastes and lime-based mortars was studied incorporating FC at dosages of 0%, 0.1%, 0.2% and 0.3 wt% by weight of binder. The lime pastes were subjected to thermal and nitrogen gas sorption analyses to understand if FC affects the formation of hydraulic compounds and the mesoporosities volume and distribution. The setting and early hydration of the mortars were studied with isothermal calorimetry. The mechanical performances were investigated with compressive and three-point-bending tests. Furthermore, fragments resulting from the mechanical tests were microscopically studied to understand the reinforcement mechanism of the fibres. It was found that 0.3 wt% of FC enhances the flexural and compressive strengths respectively by 57% and 44% while the crack propagation after the material failure is not affected.

lime mortar fibre reinforced concrete natural fibres cellulose

1. Introduction

Cement is the most widely used building material and its production is responsible for a large share of greenhouse gas emissions. It has been estimated that cement production can be accounted for about 5% of the total anthropogenic CO_2 emissions and averagely 12–15% of the industrial energy consumption of each country [1][2][3]. For this reason, several efforts have been directed on reducing the environmental impact of concrete e.g., replacing or blending ordinary Portland cement with alternative binders or using eco-friendly additives.

The use of fibres in mortars and concrete can help to enhance the properties of the final composites. Natural fibres were commonly employed during ancient times to reinforce and to reduce the shrinkage in mortars and concrete; nowadays their application in modern composites is newly evaluated as they represent a renewable, economical and abundant resource [4] and can become an alternative to the use of other synthetic fibres.

Nanocellulose materials can overall enhance the mechanical properties of modern concrete due to their high aspect ratio and high Young's modulus [5][6][7]. Moreover, due to their high hygroscopicity they can act as an internal curing agent of cement, preventing self-desiccation and promoting hydration as well as autogenous healing phenomena [8][9][10]. Their application as viscosity modifiers in self-compacting concrete (SCC) allows to stabilise the fresh concrete, inhibiting bleeding and segregation phenomena [11]. Cellulose fibres in concrete can also help tuning the composite porosity and changing its hygrothermal behaviour [12][13][14]. On the other hand, some

disadvantages must be considered, e.g., the incorporation of this kind of fibres can highly decrease the workability of the fresh concrete, making the casting process more difficult. Moreover, the results in literature are highly scattered [15] as they strongly depend on the nature of the cellulose fibres employed: the source (e.g., plant, waste materials, bacteria), their production process and the strategy of incorporation used.

The use of nanocellulose in traditional lime-based mortars is a promising solution for green buildings in the frame of limiting the CO_2 emissions resulting from Portland Cement production [16]. Unlike ordinary Portland cement, lime is fired at lower temperatures (below 1000 °C), causing less CO_2 emissions. Additionally, slaked lime partially re-absorbs the carbon dioxide emitted during the production process as it recarbonates over its in-use phase, thus resulting in lower net carbon emissions [17][18]. Moreover, lime can as well be used for the retrofit of historical buildings [19], since it is well known that cement-based mortars are not chemically and physically compatible with aged and porous materials [20]. In this context, the use of fibres can indeed help increasing the flexural strength, avoiding crack propagation in mortars and plasters, eventually delaying the need for maintenance interventions. However, to our knowledge, no extensive study of the influence of nano- and micro-fibrillated cellulose materials on the hydration and on the mechanical properties of lime-based mortars has been performed so far.

2. Fibrillated Cellulose on Lime Pastes and Mortars

2.1. Fibrillated Cellulose

The fibres used in this study are composed of a complicated network (**Figure 1**), as observed in the scanning electron microscope (SEM) images. The primary fibre diameters are below 30 nm, but due to the partial defibrillation bigger bundles of fibres were observed. The aspect ratio is high as the fibre length is in the micrometric scale: however, it was not possible to get an accurate average of the fibre lengths, due to the complicated network they form.

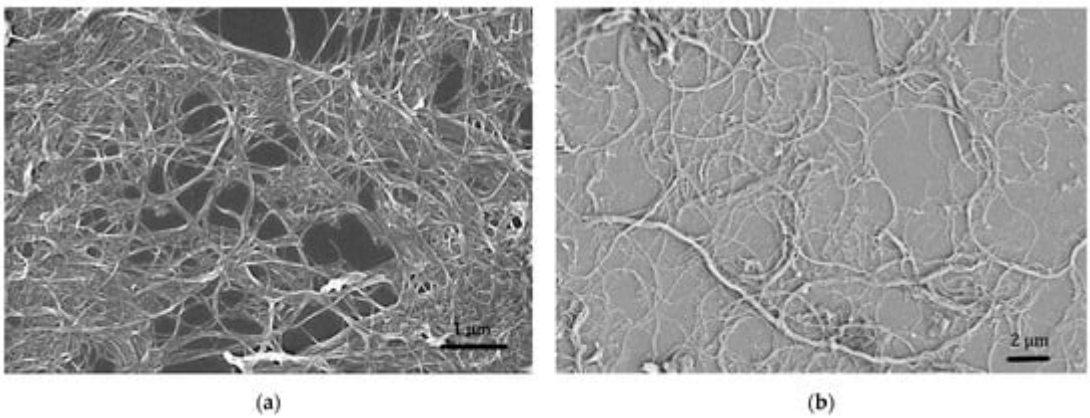

Figure 1. SEM images at different magnifications of a sample of new Celova produced by Weidmann, Switzerland with SE InLens (**a**) and normal SE (**b**) detector; bundles of cellulose fibres above 100 nm arise all over the sample.

The water retention value ranges between 1500% and 2000% per mass of dry cellulose (**Figure 2**). The loss in workability experienced in preparing the mortars and the required increase in the SP content to obtain similar slumps are thus not only due to the complex 3D net of the FC but also to the high amount of water absorbed by the cellulose. However, since the mechanism of water release is still not clear, the absorbed water was not subtracted from the calculation of the total water to binder ratio.

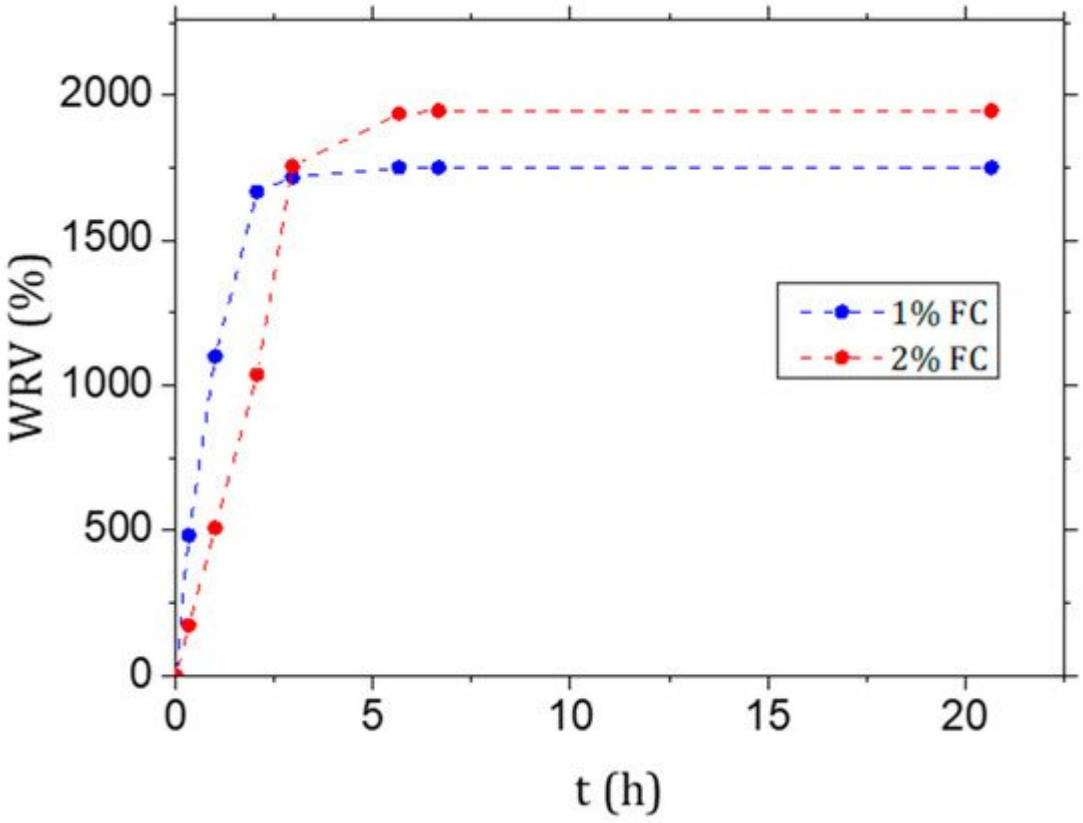

Figure 2. Water retention value (WRV%) of the fibrillated cellulose (FC) gel used to cast the samples diluted to 1% and 2% *w*/*w*.

2.2. Hydration Study

Hydraulic lime mainly sets by the reaction of dicalcium silicate (C_2S) with water to form calcium silicate hydrates (*CSH*); some hydrated lime (free lime) is also formed in addition to the one already present in the powder before the reaction (Equation (1))

$$C_2S + \mathrm{H_2O} \rightarrow CSH + \mathrm{Ca(OH)_2}$$

The lime paste is highly alkaline, but this condition changes progressively on aging because carbon dioxide starts penetrating into the system once the paste is set and transforms the hydrated lime into calcium carbonate. Carbon dioxide also reacts with the hydrated calcium silicate forming calcium carbonate and amorphous silica (*SH*) (Equation (2)).

$$CSH + \mathrm{Ca(OH)_2} + \mathrm{CO_2} \rightarrow \mathrm{CaCO_3} + SH + \mathrm{H_2O}$$

As the introduced FC has a high WRV%, it was crucial to understand if the setting and hardening reactions in the lime pastes could be affected; more specifically emphasis was put in understanding if the formation of *CSH*, important for the final mechanical strength of the mortar, was inhibited or delayed. It has been discussed that in Portland cement-based mortars and concretes, natural fibres can slow down the hydration at early stages, but natural fibres can also act as an internal reservoir of water avoiding the desiccation of composites and therefore at last promoting the hydration of mortars [9].

The XRD pattern (**Figure 3**) at 2 d and after 28 d show in all four samples a gradual decrease in the Portlandite content, while at the same time the peaks assigned to calcite increase in intensity. The signals associated to the formation of the hydrates (*CSH* and *CAH* in the form of katoite) slowly increase, too.

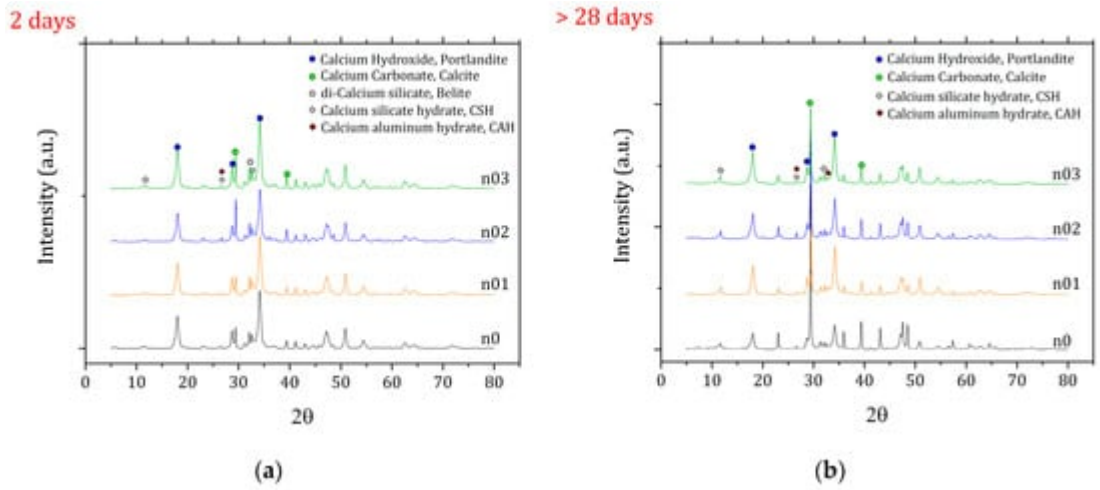

Figure 3. XRD pattern of the four pastes at 2 d (**a**) and after 28 d of curing (**b**).

To obtain a quantitative impression of the pastes composition, thermogravimetric analyses (TGA) were performed. The TGA curves show that the formation rate of the hydrates is comparable in all the four samples examined. After 21 d of curing the mass loss between 105 °C and 370 °C fluctuates around 4.5% of the total mass up to 45 d. The fractions of portlandite and of calcite, on the other hand, are different in the samples with and without fibres. In samples with fibres the decrease in portlandite and the increase in the calcite content seem to be slower. At 45 d of curing the LdX for n0 is near 4% and between 5.3% and 6.5% for n01, n02 and n03, while LdC is over 22% for n0 and below 18% for n01, n02 and n03. Further studies at different relative humidities should be conducted to understand if FC can play a role in CO_2 penetration by affecting the paste porosity or if the water stored in the FC can indeed delay the carbonation by avoiding the self-desiccation.

2.3. Nitrogen Gas Sorption

The calculated specific surface area for the lime pastes n0, n01, n02 and n03 ranges between 9 m^2/g and 11 m^2/g without a significant difference within the accuracy of the measurements. The pores volume distribution is also very similar among the series with the exception of n03 for which the mesoporosities are lower in the range of 20–70 nm (**Figure 4**). Moreover, the mortars show a similar trend, but the presence of aggregates and inhomogeneities of the

samples leads to a higher scatter in the results. These results could indicate that the fibres partially reduce the mesoporosities of the composite.

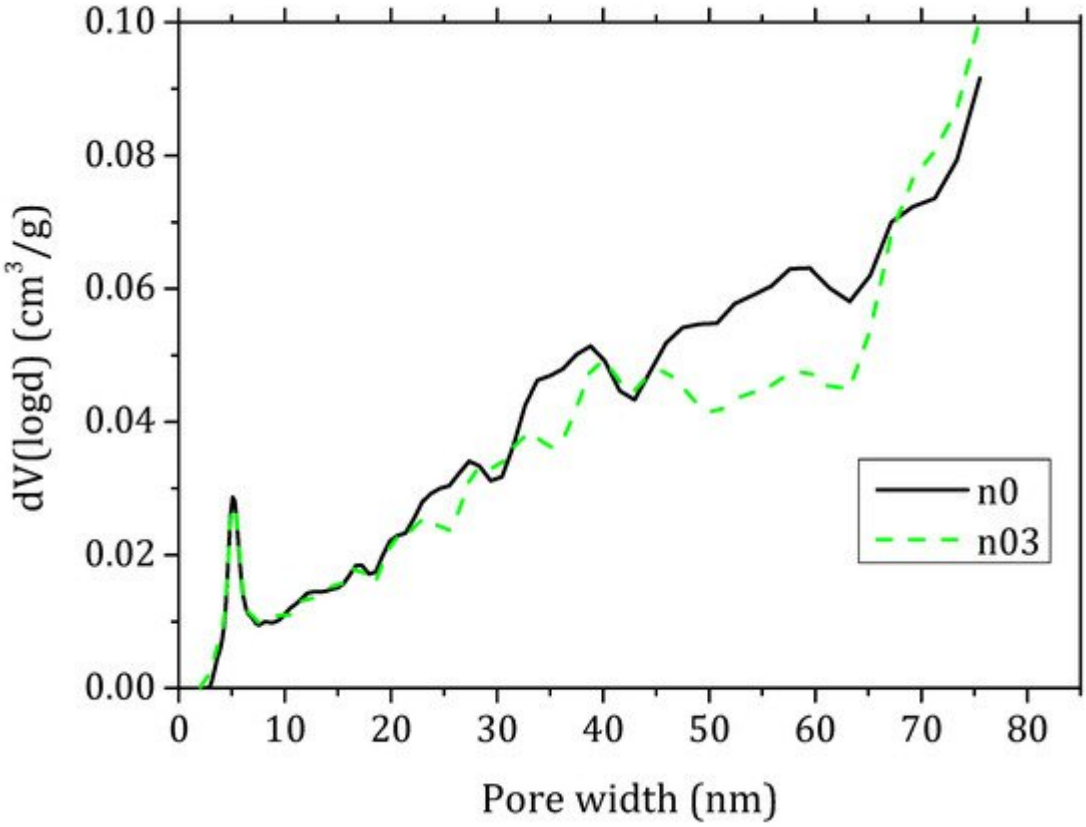

Figure 4. Pore size distribution calculated by DFT method from N_2 adsorption–desorption isotherms for lime pastes with 0% FC (n0) and 0.3% fc (n03).

2.4. Isothermal Calorimetry

The specific heat development per gram of binder is presented in **Figure 5**. A maximum is observed after 1 h. The rapid increase in the heat release can be connected to the heat of wetting [21]. A retardant effect on the setting hydration of cement mortars connected to the use of PCE was often reported [22][23]; this phenomenon was not observed in our lime mixes, despite the difference in the superplasticiser content. On the contrary a slight shift on the left was observed for N02 and N03, the samples with higher superplasticiser content. The maximum heat rate value is higher in samples with FC and could be connected to the partial alkaline hydrolysis of the cellulose by peeling [24]. However, the curve associated to N0 is broader and the cumulative heat recorded is higher.

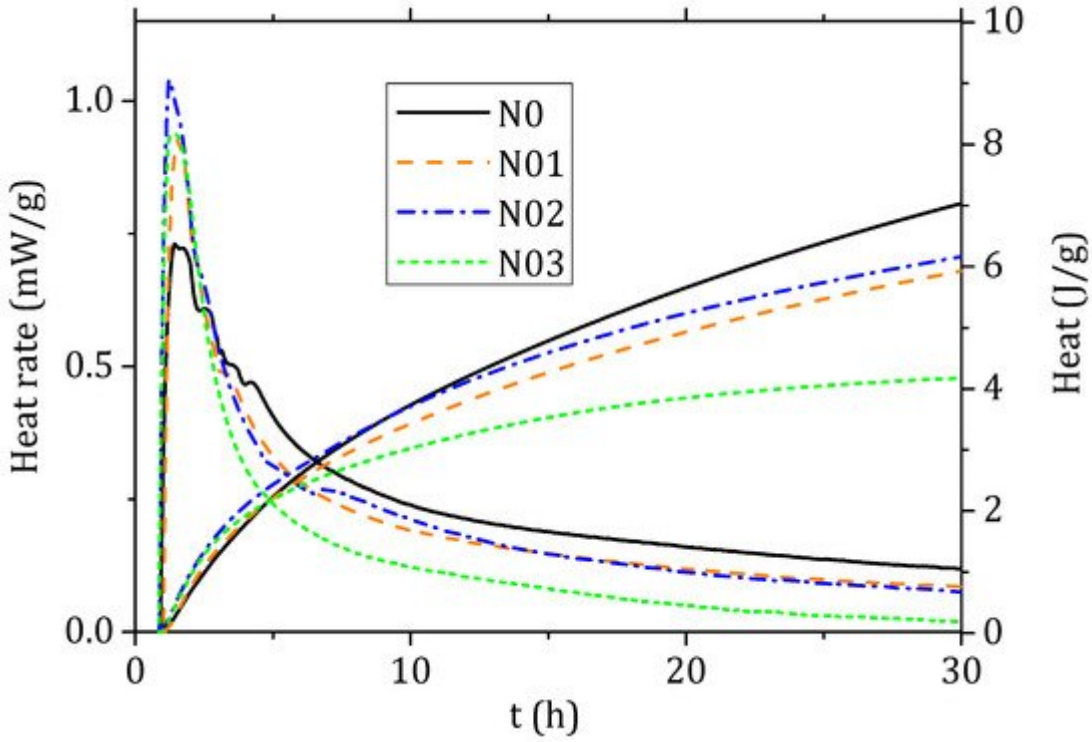

Figure 5. Isothermal calorimetry results for the four different mortar mixtures expressed in heat rate (mW) and heat (J) normalised to the mass of binder.

2.5. Mechanical Tests

Preliminary tests showed that 0.1% and 0.2% FC affect less significantly the mechanical properties of the mortars, in particular the compression strength (**Figure 6**). Therefore, the study focused on the comparison between the 0% and 0.3% FC mixtures. Each mix was casted three times to increase the statistics, reduce the dispersion of data (typical of this kind of building materials) and understand the reproducibility of the results. For each mix, 10 and 15 samples were tested respectively at 28 d and at 45 d. The results from the mechanical tests in terms of flexural strength (f_{fl}) and compression strength (f_c) are respectively shown in **Table 1** and **Table 2**. The flexural and compression strength in samples with 0.3% FC are improved respectively by 47% and 41% at 28 d and by 50% and 42% at 45 d (**Figure 7**).

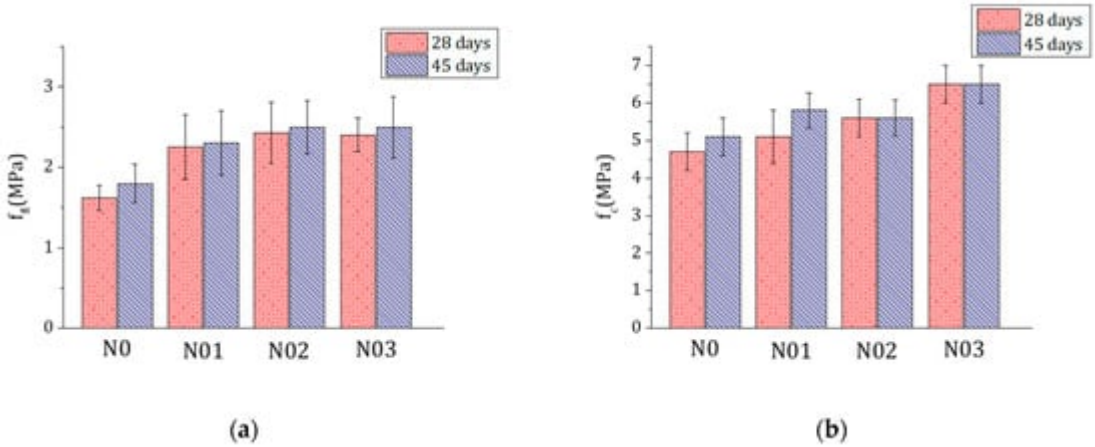

Figure 6. Flexural strength f_{fl} (**a**) and compression strength f_c (**b**) of samples with 0% (N0), 0.1% (N01), 0.2% (N02) and 0.3% FC (N03) at 28 d (red) and 45 d (blue).

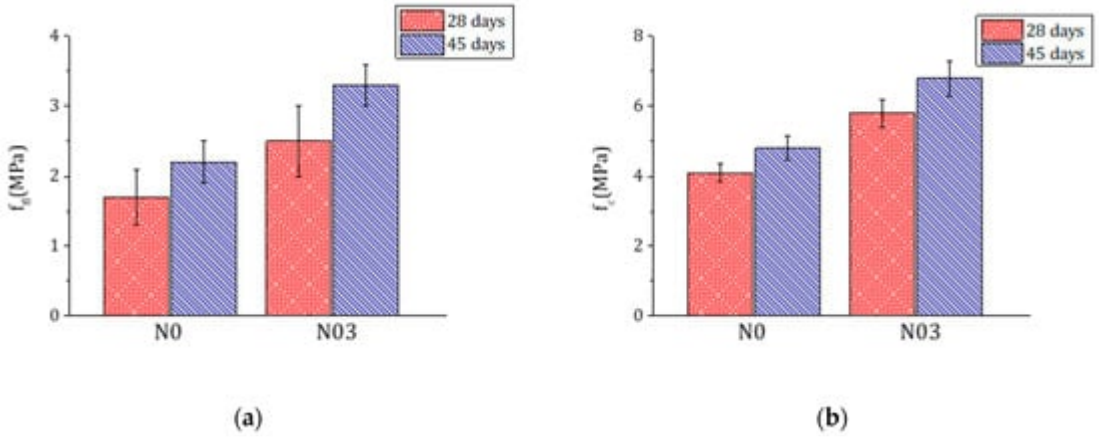

Figure 6. Flexural strength f_{fl} (**a**) and compression strength f_c (**b**) of samples with 0% FC (N0) and 0.3% FC (N03) at 28 d (red) and 45 d (blue).

Table 1. Flexural strength (f_{fl}) of samples with 0% FC (N0) and 0.3% FC (N03).

Mix	Day 28	Day 45
N0	1.7 ± 0.4	2.2 ± 0.3
N03	2.5 ± 0.5	3.3 ± 0.3

Table 2. Compression strength (f_c) of samples with 0% FC (N0) and 0.3% FC (N03).

Mix	Day 28	Day 45
N0	4.1 ± 0.3	4.8 ± 0.3
N03	5.8 ± 0.4	6.8 ± 0.5

Representative experimental flexural stress–strain curves are shown in **Figure 8** and were analysed to understand if the fibres also affect the brittle behaviour of the material. The total area under the three-point-bending test curve is also improved in N03 (**Table 3**). On the other hand, Ab and εb are not significantly affected by the FC, so that the fibres seem to have little effect on the post-crack behaviour and deflection of the composite. The flexural elastic modulus E, on the contrary, is enhanced by 54% indicating the material is behaving in a more rigid way.

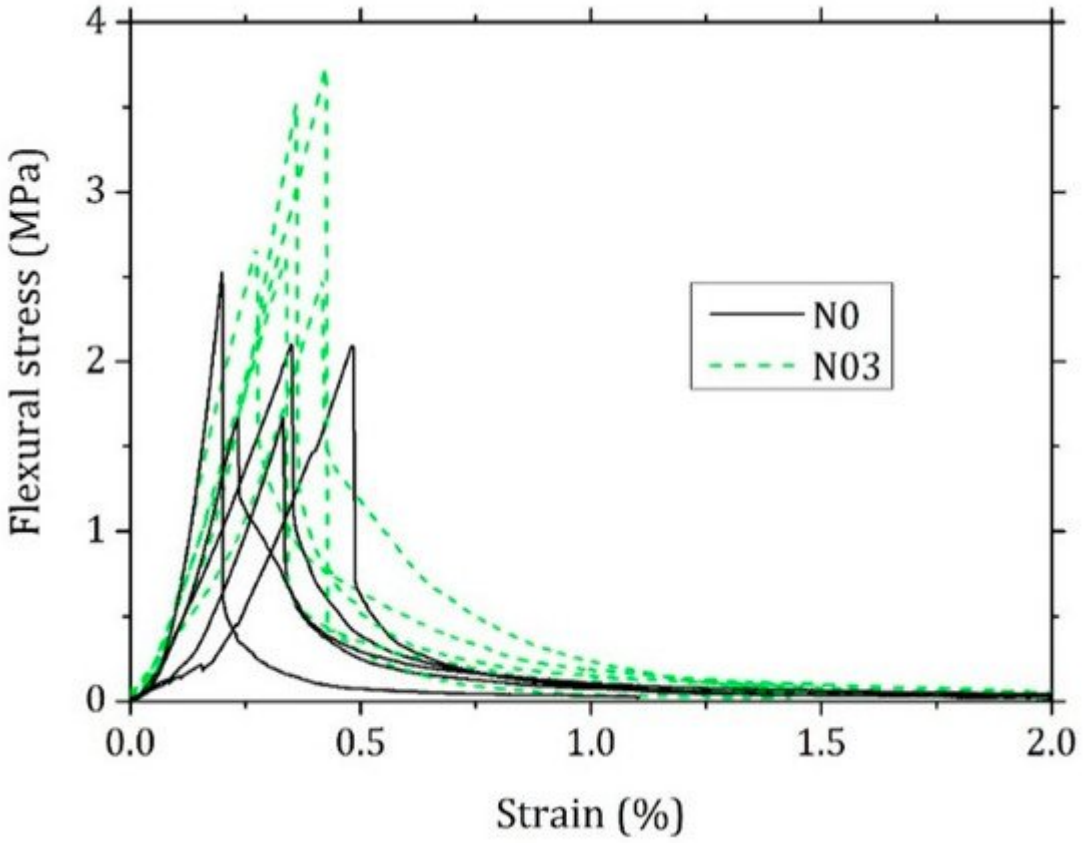

Figure 8. Representative flexural stress–strain curves from the three-point-bending test for samples with 0% (N0) and 0.3% (N03) FC.

Table 3. Results of three-point bending test stress–strain curves: total area (A) of the stress (MPa)-strain (%) relation, area (A_b) after the break point (ε_b) and flexural modulus (E) of mortars with 0% FC (N0) and 0.3% FC (N03).

Mix	A (MPa%)	A_b (MPa%)	ε_b (%)	E (MPa)
N0	0.6 ± 0.1	0.22 ± 0.07	0.48 ± 0.04	641 ± 113
N03	0.8 ± 0.1	0.31 ± 0.07	0.42 ± 0.04	986 ± 104

The FC effect on the mechanical properties can be connected to the microstructural changes that the fibres can induce in composites and that were already observed in Portland cement concrete. These changes can be due to the higher elastic modulus of the crystalline portion of cellulose nanomaterials (usually in the range of 100–130 GPa) [25], their high specific surface area and the interaction of the surface –OH groups with *CSH* and portlandite that leads to a strong fibre–matrix bonding, which involves a better stress transfer from the matrix to the nanofibers, but in return can also cause an excessive embrittlement of the composite [26][27].

The Weibull statistics was applied on the data of the mechanical strength at 45 d (**Figure 9**), a time at which, in the frame of our work, the mortars reached the highest strength. The Weibull analysis confirms the overall enhancement of the mechanical properties (**Table 4**) determined by the fibres, and the characteristic strength σ_0 is close to the normal distribution averages calculated. The flexural and compressive σ_0 in the N03 series are enhanced respectively by 57% and 44%. The Weibull modulus m of the flexural data is considerably higher in samples with 0.3% fibre content, indicating that the distribution is narrower and the results less scattered. A higher Weibull modulus is indeed usually more desirable as the material has a lower probability to fail at a stress much lower than σ_0.

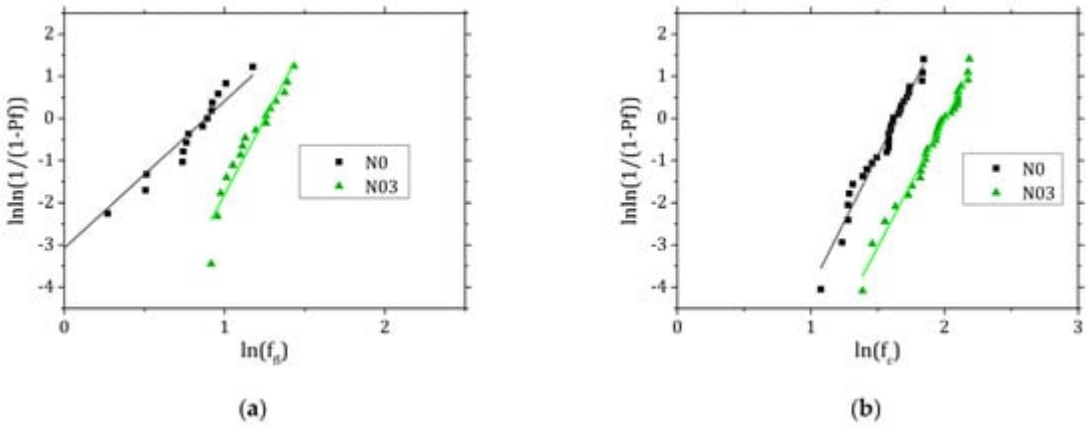

Figure 9. Linear fit of the experimental data from the three-point bending (**a**) and compression (**b**) tests analysed with Weibull statistics.

Table 4. Average experimental strength values and parameters obtained after Weibull fitting.

Mix	f_{fl} (MPa)	Flexural σ_0 (MPa)	m	R^2
N0	2.2	2.3	4.1	0.93
N03	3.3	3.6	7.0	0.94
	f_c (MPa)	**Compressive σ_0 (MPa)**	**m**	**R^2**
N0	4.8	5.2	6.3	0.97
N03	6.8	7.5	6.1	0.98

2.6. Microscopic Observation

Optical microscope observations (**Figure 10**) showed that both N0 and N03 are homogeneous, and the aggregate is well dispersed in the binder. On the other hand, the samples with FC seem to have less voids and cracks as the embedding resin did not penetrate as much as in N0.

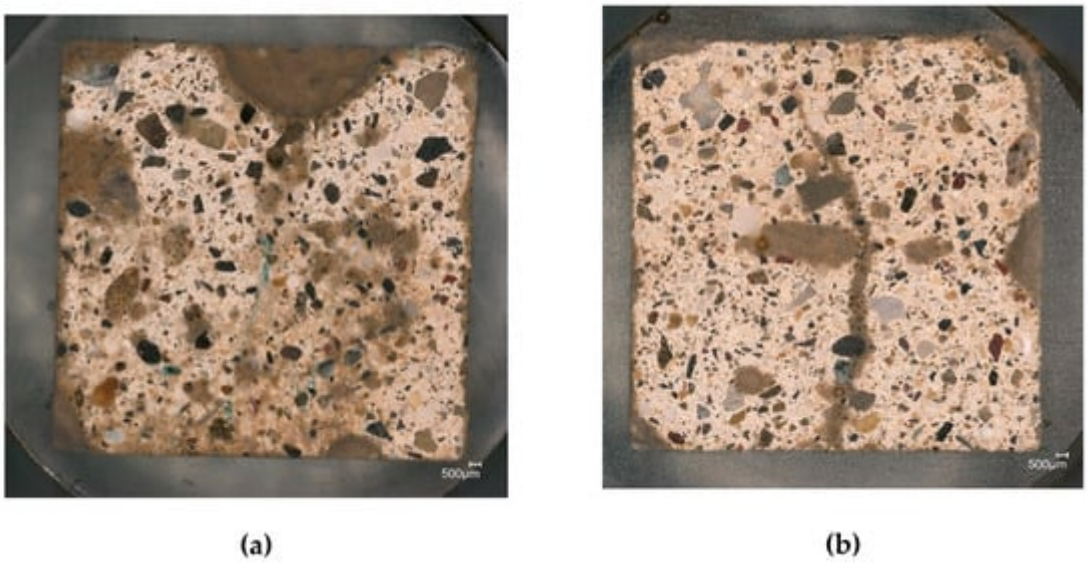

Figure 10. Embedded samples with 0% FC (**a**) and 0.3% FC (**b**) prior to the carbon coating observed with an optical microscope.

SEM images confirm that a content of 0.3% fibrillated cellulose increases the compactness of the mortar, by reducing the presence of voids. Additionally, the aggregate to binder interphase, the interfacial transition zone (ITZ), appears to be also improved (**Figure 11**). The ITZ is considered the weakest element of mortars and concretes, as the first cracks leading to material failure generally originate there. Therefore, a better interaction between binder and aggregate can lead to an enhancement of mechanical properties. Moreover, the general reduction of cracks and voids may improve the durability of the material, as cracks can be the main point of entry for water or aggressive chemical ions [28]. The FC effect in strengthening the ITZ and reducing the crack formation has already been observed in Portland cement concrete [12]. For the materials described in this work these aspects may as well be connected to the tendency that the filaments have to form a 3D network (**Figure 1**). This effect was also described elsewhere upon application of similar cellulose materials [11]. In this proposed reinforcement mechanism, the key to have a significant effect of the fibres is the formation of a continuous network that connects the particles in the mortar. This mechanism would also explain why lower loads of fibres do not significantly improve the mechanical strength of the resulting materials. On the other hand, no clear evidence of a bridging effect by the FC was found. It must be noted, though, that given the fibre morphology and size, it is extremely complicated to confidently distinguish them from the hydraulic compounds formed during lime hydration (**Figure 12**).

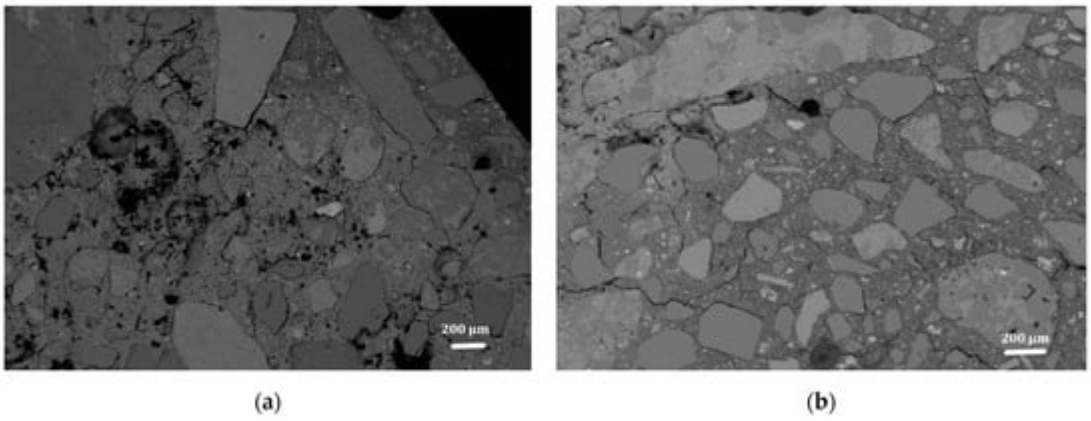

Figure 11. Backscattered electron (BSE) SEM images of mortars with 0% FC (**a**) and 0.3% FC (**b**).

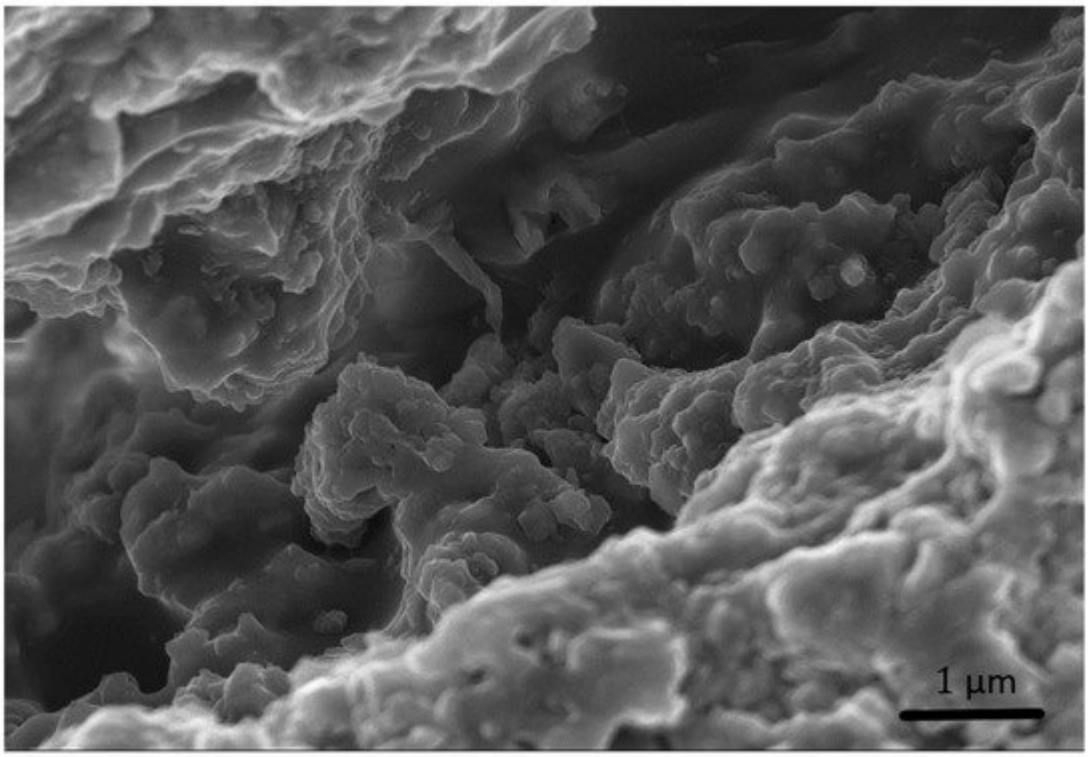

Figure 12. Secondary electron (SE) SEM image of a possible filament of cellulose detected in a crack and immersed in the forming gel.

The 3D topographies of the fractured surfaces of four representative samples are shown in **Figure 13**. The roughness parameters describing the two series are similar (**Table 5**). The calculated skewness shows that the peaks and valleys are normally distributed as the values are close to 0. The Sku for N0 defines that the distribution has a more collapsed shape. Overall, though, the 3D topographic images and the surface roughness parameters calculated did not underline any remarkable difference among the two series.

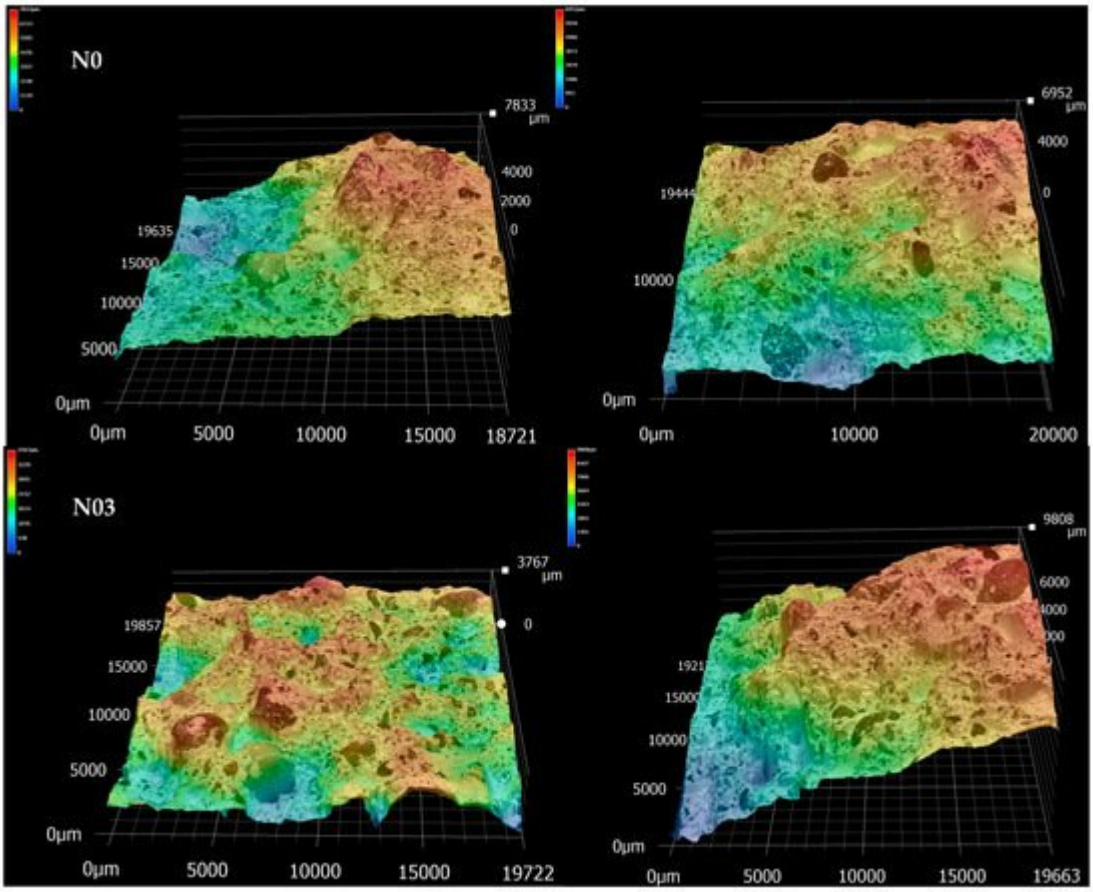

Figure 13. Representative 3D topographic images (20 mm × 20 mm ca) of the mortars fractured surfaces with 0% FC (N0) and 0.3% FC (N03).

Table 5. Average surface roughness values obtained from 3D scans of fractured surfaces after three-point-bending tests.

Mix	*Sa* (µm)	*Sz* (µm)	*Sq* (µm)	*Ssk* (µm)	*Sku* (µm)
N0	1110 ± 322	6450 ± 1445	1341 ± 381	0.1 ± 0.2	2.4 ± 0.3
N03	1157 ± 352	6472 ± 1219	1324 ± 405	0.1 ± 0.4	2.7 ± 0.5

References

1. Madlool, N.A.; Saidur, R.; Hossain, M.S.; Rahim, N.A. A critical review on energy use and savings in the cement industries. Renew. Sustain. Energy Rev. 2011, 15, 2042–2060.
2. Summerbell, D.L.; Barlow, C.Y.; Cullen, J.M. Potential reduction of carbon emissions by performance improvement: A cement industry case study. J. Clean. Prod. 2016, 135, 1327–1339.

3. Thwe, E.; Khatiwada, D.; Gasparatos, A. Life cycle assessment of a cement plant in Naypyitaw, Myanmar. Clean. Environ. Syst. 2021, 2, 100007.
4. Ma, W.; Qin, Y.; Li, Y.; Chai, J.; Zhang, X.; Ma, Y.; Liu, H. Mechanical properties and engineering application of cellulose fiber-reinforced concrete. Mater. Today Commun. 2020, 22, 100818.
5. Fu, T.; Moon, R.J.; Zavattieri, P.; Youngblood, J.; Weiss, W.J. Cellulose nanomaterials as additives for cementitious materials. In Cellulose-Reinforced Nanofibre Composites; Elsevier Ltd.: Amsterdam, The Netherlands, 2017; Volume C, pp. 455–482. ISBN 9780081009659.
6. Hisseine, O.A.; Omran, A.F.; Tagnit-Hamou, A. Influence of cellulose filaments on cement paste and concrete. J. Mater. Civ. Eng. 2018, 30, 04018109.
7. Cengiz, A.; Kaya, M.; Pekel Bayramgil, N. Flexural stress enhancement of concrete by incorporation of algal cellulose nanofibers. Constr. Build. Mater. 2017, 149, 289–295.
8. Fu, T.; Montes, F.; Suraneni, P.; Youngblood, J.; Weiss, J. The influence of cellulose nanocrystals on the hydration and flexural strength of Portland cement pastes. Polymers 2017, 9, 424.
9. Onuaguluchi, O.; Panesar, D.K.; Sain, M. Properties of nanofibre reinforced cement composites. Constr. Build. Mater. 2014, 63, 119–124.
10. Snoeck, D.; Smetryns, P.A.; De Belie, N. Improved multiple cracking and autogenous healing in cementitious materials by means of chemically-treated natural fibres. Biosyst. Eng. 2015, 139, 87–99.
11. Hisseine, O.A.; Basic, N.; Omran, A.F.; Tagnit-Hamou, A. Feasibility of using cellulose filaments as a viscosity modifying agent in self-consolidating concrete. Cem. Concr. Compos. 2018, 94, 327–340.
12. Barnat-Hunek, D.; Szymańska-Chargot, M.; Jarosz-Hadam, M.; Łagód, G. Effect of cellulose nanofibrils and nanocrystals on physical properties of concrete. Constr. Build. Mater. 2019, 223, 1–11.
13. Collet, F.; Chamoin, J.; Pretot, S.; Lanos, C. Comparison of the hygric behaviour of three hemp concretes. Energy Build. 2013, 62, 294–303.
14. Mejdoub, R.; Hammi, H.; Suñol, J.J.; Khitouni, M.; M'nif, A.; Boufi, S. Nanofibrillated cellulose as nanoreinforcement in Portland cement: Thermal, mechanical and microstructural properties. J. Compos. Mater. 2017, 51, 2491–2503.
15. Balea, A.; Fuente, E.; Blanco, A.; Negro, C. Nanocelluloses: Natural-based materials for fiber-reinforced cement composites. A critical review. Polymers 2019, 11, 518.
16. Ip, K.; Miller, A. Life cycle greenhouse gas emissions of hemp-lime wall constructions in the UK. Resour. Conserv. Recycl. 2012, 69, 1–9.

17. Kang, S.-H.; Kwon, Y.-H.; Moon, J. Quantitative Analysis of CO2 Uptake and Mechanical Properties of Air Lime-Based Materials. Energies 2019, 12, 2903.
18. SAINT-ASTIER Preservation of Our Built Heritage: St. Astier NHL Mortars. Available online: http://www.stastier.co.uk/articles/preserving-heritage.htm (accessed on 23 November 2021).
19. Filippi, M. Remarks on the green retrofitting of historic buildings in Italy. Energy Build. 2015, 95, 15–22.
20. Kang, S.H.; Lee, S.O.; Hong, S.G.; Kwon, Y.H. Historical and scientific investigations into the use of hydraulic lime in Korea and preventive conservation of historic masonry structures. Sustainability 2019, 11, 5169.
21. Jerman, M.; Tydlitát, V.; Keppert, M.; Čáchová, M.; Černý, R. Characterization of early-age hydration processes in lime-ceramic binders using isothermal calorimetry, X-ray diffraction and scanning electron microscopy. Thermochim. Acta 2016, 633, 108–115.
22. Flatt, R.; Schober, I. Superplasticizers and the Rheology of Concrete; Woodhead Publishing Limited: Cambrige, UK, 2012.
23. Marchon, D.; Flatt, R.J. Impact of Chemical Admixtures on Cement Hydration; Woodhead Publishing, Elsevier Ltd.: Amsterdam, The Netherlands, 2016; ISBN 9780081006962.
24. Knill, C.J.; Kennedy, J.F. Degradation of cellulose under alkaline conditions. Carbohydr. Polym. 2003, 51, 281–300.
25. Dufresne, A. Nanocellulose: A new ageless bionanomaterial. Mater. Today 2013, 16, 220–227.
26. Hisseine, O.A.; Wilson, W.; Sorelli, L.; Tolnai, B.; Tagnit-Hamou, A. Nanocellulose for improved concrete performance: A macro-to-micro investigation for disclosing the effects of cellulose filaments on strength of cement systems. Constr. Build. Mater. 2019, 206, 84–96.
27. Ardanuy, M.; Claramunt, J.; Arévalo, R.; Parés, F.; Aracri, E.; Vidal, T. Nanofibrillated cellulose (Nfc) as a potential reinforcement for high performance cement mortar composites. BioResources 2012, 7, 3883–3894.
28. Kockal, N.U.; Ozturan, T. Effects of lightweight fly ash aggregate properties on the behavior of lightweight concretes. J. Hazard. Mater. 2010, 179, 954–965.